Mon. Not. R. Astron. Soc. **000**, 000–000 (0000) Printed 29 April 2014 (MN LATEX style file v2.2)

# Beyond Halo Mass: Galactic Conformity as a Smoking Gun of Central Galaxy Assembly Bias

Andrew P. Hearin[1,2,3], Douglas F. Watson[2,⋆] & Frank C. van den Bosch[4]
[1] *Fermilab Center for Particle Astrophysics, Fermi National Accelerator Laboratory, Batavia, IL*
[2] *Kavli Institute for Cosmological Physics, 5640 South Ellis Avenue, The University of Chicago, Chicago, IL*
[3] *Yale Center for Astronomy & Astrophysics, Yale University, New Haven, CT*
[4] *Department of Astronomy, Yale University, P.O. Box 208101, New Haven, CT*

arXiv:1404.6524v1 [astro-ph.CO] 25 Apr 2014

29 April 2014

**ABSTRACT**

Quenched central galaxies tend to reside in a preferentially quenched large-scale environment, a phenomenon that has been dubbed *galactic conformity*. Remarkably, this tendency persists out to scales far larger than the virial radius of the halo hosting the central. Therefore, conformity manifestly violates the widely adopted assumption that the dark matter halo mass $M_{\rm vir}$ exclusively governs galaxy occupation statistics. This paper is the first in a series studying the implications of the observed conformity signal for the galaxy-dark matter connection. We show that recent measurements of conformity on scales $r \sim 1-5$ Mpc imply that central galaxy quenching statistics cannot be correctly predicted with the knowledge of $M_{\rm vir}$ alone. We also demonstrate that ejected (or 'backsplash') satellites cannot give rise to the signal. We then invoke the age matching model, which is predicated on the co-evolution of galaxies and halos. We find that this model produces a strong signal, and that central galaxies are solely responsible. We conclude that large-scale '2-halo' conformity represents a smoking gun of *central galaxy assembly bias,* and indicates that contemporary models of satellite quenching have systematically over-estimated the influence of post-infall processes.

**Key words:** cosmology: theory — dark matter — galaxies: halos — galaxies: evolution — galaxies: clustering — large-scale structure of universe

## 1 INTRODUCTION

The well-established connection between galaxies and dark matter halos forms the basis of a very broad class of models of galaxy evolution that we will loosely refer to as halo occupation models. Such models exploit the ability of contemporary N-body simulations to calculate the abundance, spatial distribution, and internal structure of dark matter halos with exquisite precision. Armed with this knowledge, halo occupation models make predictions for the observed galaxy distribution by specifying, in a statistical sense, how galaxies populate dark matter halos.

The Halo Occupation Distribution (HOD, e.g., Seljak 2000; Berlind & Weinberg 2002; Zheng et al. 2005) and the closely related Conditional Luminosity Function (CLF, e.g., Yang et al. 2003; van den Bosch et al. 2013) are the two most prevalent classes of halo occupation models in the literature. In the HOD, the galaxy-halo connection is formalized by the quantity $P(N_{\rm gal}|M_{\rm vir})$, the probability that a halo of mass $M_{\rm vir}$ hosts $N_{\rm gal}$ galaxies brighter than some luminosity (or stellar mass) threshold. In the CLF, the quantity $\Phi(\mathrm{L}|M_{\rm vir})$ plays the central role by specifying the mean abundance of galaxies of luminosity $L$ found in dark matter halos of mass $M_{\rm vir}$. These well-studied formalisms have both proven to be very powerful theoretical tools to constrain both the galaxy-halo connection (see, for example, Magliocchetti & Porciani 2003; Yang et al. 2003; Zehavi et al. 2005; Cooray 2006; Zheng et al. 2007; van den Bosch et al. 2007; Zheng et al. 2009; Skibba & Sheth 2009; Simon et al. 2009; Ross et al. 2010; Zehavi et al. 2011; Watson et al. 2011; Tinker et al. 2013, and references therein) and the fundamental parameters in cosmology (van den Bosch et al. 2003; Tinker et al. 2005; Leauthaud et al. 2011; More et al. 2013; Cacciato et al. 2013).

⋆ NSF Astronomy & Astrophysics Postdoctoral Fellow

© 0000 RAS

All of the above results concerning both cosmology and galaxy evolution are predicated upon the assumption that the mass $M_{\rm vir}$ of a dark matter halo entirely determines the statistical properties of its resident galaxy population. Yet, it is well established that the spatial distribution of dark matter halos depends on halo properties besides mass (Gao et al. 2005; Wechsler et al. 2006; Gao & White 2007; Wetzel et al. 2007; Dalal et al. 2008; Li et al. 2008; Lacerna & Padilla 2011, 2012). Here we will collectively refer to the dependence of halo clustering upon additional halo properties besides $M_{\rm vir}$ as *halo assembly bias*. Of course, if galaxy occupation statistics depend only on $M_{\rm vir}$, then halo assembly bias only contributes random noise in halo model predictions for the galaxy distribution.

Because halo occupation models such as the HOD and CLF have generally been very successful at fitting observations of galaxy clustering statistics, the possibility that the galaxy-halo connection requires dependence on additional parameters besides $M_{\rm vir}$ is generally not considered. However, it has recently been shown in Zentner et al. (2013) that this assumption has the potential to introduce significant systematic errors in halo occupation modeling of the two-point clustering of luminosity threshold galaxy samples. Zentner et al. (2013) showed that these systematics can be even more severe when color cuts comprise part of the selection function, such as, for example, in halo occupation modeling of color-dependent clustering (e.g., Zehavi et al. 2011). In what follows, we will generically refer to any dependence of the mapping between galaxies and halos upon halo properties besides $M_{\rm vir}$ as *galaxy assembly bias*. In particular, our focus in this paper will be the potential correlation of galaxy color/star formation rate with halo properties besides $M_{\rm vir}$.

In the context of assembly bias, galaxy group catalogs constructed from large redshift surveys, such as the Sloan Digital Sky Survey (SDSS: York et al. 2000; Abazajian et al. 2009), have proven to be particularly rich datasets. For example, in Weinmann et al. (2006, hereafter W06), the authors used the halo-based group-finding algorithm of Yang et al. (2005) to divide their SDSS galaxy sample into *central* galaxies residing at the center of the dark matter halo of the group, and *satellite* galaxies orbiting around the central within the potential well of the group's halo. W06 found that both the $g-r$ color and star formation rate (SFR) of satellite galaxies depends on the color/SFR of the group's central galaxy at fixed halo mass,[1] a phenomenon the authors dubbed *galactic conformity*.[2] If correct, this observation manifestly violates the assumption that galaxy assembly bias is zero, as the properties of the satellites were explicitly shown to have an additional dependence upon some property besides $M_{\rm vir}$ (in particular, satellite color/SFR evidently also depends on the color/SFR of the central).

In a recent, closely related paper, Kauffmann et al. (2013, hereafter K13) used SDSS data to demonstrate that correlations between star formation indicators of central galaxies and their neighboring galaxies persist out to several Mpc, far outside the virial radius of the host halos of the centrals. Although K13 also used the term "conformity" to refer to the signal they measured, from the perspective of the halo model (e.g., Cooray & Sheth 2002; Mo et al. 2010) the W06 and K13 measurements are qualitatively distinct: the former refer to SFR correlations between galaxies occupying the same dark matter halo, while the latter considers galaxies in distinct halos. Hence, in what follows we refer to the conformity signals detected by W06 and K13 as "1-halo" and "2-halo" conformity, respectively.

This paper is the first in a series investigating the implications of galactic conformity for halo occupation statistics and for the physics of galaxy formation (in particular galaxy quenching). In this paper we argue that *central* galaxy assembly bias is required for any galaxy-halo model to produce non-zero 2-halo conformity. In a companion paper to the present work (Paper II), we will show that 1-halo conformity can naturally be encoded in a generalized HOD formalism, and demonstrate that the W06 measurements indicate that this signal is strong enough to significantly impact small-scale clustering. Each of these two "theory papers" will be accompanied by its own follow-up paper providing new measurements of the corresponding conformity signal. In the observational follow-up to the present paper (Paper III), we will quantitatively compare our updated K13 measurements to predictions from both empirical and semi-analytic models (SAMs) of galaxy formation, and seek to identify the ingredients necessary to bring theoretical predictions into accord with the observations. Finally, in Paper IV, we will conduct a likelihood analysis using the generalized HOD model developed in Paper II to provide quantitative constraints on the co-evolution of central and satellite galaxies, as well as other signatures of galaxy evolution that have been previously neglected in HOD modeling of SFR-dependent galaxy clustering.

This paper is organized as follows. We provide an overview of the conformity measurement in §2. In §3 we outline the various formulations of the galaxy-halo connection we use to model the galaxy distribution. Our primary results are presented in §4, and we discuss the implications of our findings in §5. Throughout the paper we assume a flat ΛCDM cosmological model with $\Omega_{\rm m} = 0.27$ and Hubble constant $H_0 = 70$ km s$^{-1}$ Mpc$^{-1}$.

## 2 2-HALO CONFORMITY

### 2.1 Definition of the Signal

As outlined in §1, K13 recently demonstrated that star formation indicators of central galaxies and their neighbors are correlated out to several Mpc. From a volume-limited galaxy sample constructed from the New York University Value-Added Catalog (Blanton et al. 2005),

[1] Of course the true dark matter halo mass of a galaxy group is not directly observable, and so in W06 the authors use total group luminosity as their halo mass proxy. The role played by this choice and other details associated with this conformity measurement will soon appear in Campbell et al., in prep.

[2] See also Phillips et al. (2014) for measurements of this phenomenon in a sample of satellites of isolated Milky Way-mass galaxies.

K13 first select galaxies in a specific range of stellar mass $M_*$. For a galaxy to be identified as a central, it was required that no other galaxy with stellar mass greater than $M_*/2$ lie within a projected distance of 500 kpc and a velocity difference of 500 km/s of the candidate central. Throughout this paper, we will refer to any galaxy that passes these isolation criteria as an "isolated primary". We will reserve the term "central" for galaxies that truly reside at the centers of host halos.

After applying the above isolation criteria, it was shown in K13 that when a sample of isolated primaries of the same stellar mass is divided into subsamples according to SFR, the mean specific star formation rate (defined as $\langle \mathrm{SFR}/M_* \rangle$, and written as $\langle \mathrm{sSFR} \rangle$) of galaxies neighboring quenched primaries is suppressed relative to the neighbors of primaries that are actively forming stars. As can be seen in Figs. 2 & 3 of K13, the magnitude of the effect is quite strong, and measured with high statistical significance. Moreover, for a sample of primaries with $M_* \sim 10^{10}\mathrm{M}_\odot$, K13 found that the difference in $\langle \mathrm{sSFR} \rangle$ between the samples of neighbors persists out to at least 4Mpc, *well beyond the virial radius of the host halo of the primary*. As already mentioned above, to distinguish this conformity signal from that introduced and identified by W06, we refer to this large-scale correlation between sSFRs as "2-halo conformity".

### 2.2 Significance for Halo Occupation Models of Galaxy Quenching

Non-zero 2-halo conformity represents a clear violation of the core assumption in virtually all halo occupation models, namely that galaxy properties are, in a statistical sense, governed by halo mass alone. Although a violation of this '$M_{\rm vir}$-only' ansatz is expected for some galaxy properties, such as galaxy size (which is believed to be strongly related to the halo's angular momentum: Mo et al. 1998; Kravtsov 2013), numerous studies have assumed that galaxy SFR (and hence, color) can still be modeled under the $M_{\rm vir}$-only assumption (e.g., Zehavi et al. 2005, 2011; Collister & Lahav 2005; Skibba & Sheth 2009; Tinker et al. 2013; Guo et al. 2014). Non-zero conformity not only violates one of the core assumptions on which these and other studies are based, but also has important implications for the physics of galaxy quenching. In particular, taken at face value, 2-halo conformity suggests that large-scale environment in addition to halo mass has an important impact on controlling the SFRs of individual galaxies.

However, before concluding that observed quenching statistics violate the $M_{\rm vir}$-only ansatz, it is important to verify that the conformity signal detected by K13 is not a mere manifestation of observational systematics and/or sample selection effects. For example, no isolation criterion is perfect, and so any sample of isolated primaries will be contaminated at some level by galaxies that are truly satellites. Such contamination has the potential to masquerade as 2-halo conformity for the following reason. At fixed stellar mass, it is by now well-established that satellites have a larger quenched fraction than centrals (e.g., van den Bosch et al. 2008; Wetzel et al. 2012; Watson et al. 2014). This implies that (1) when a sample of isolated primaries is divided into quenched and star-forming sub-populations, the quenched subsample will have a relatively larger fraction of contaminating satellites. Now, satellites tend to reside in more massive dark matter halos than centrals of the same stellar mass (Yang et al. 2008); halo clustering strength increases with halo mass (Mo & White 1996); and the quenched fraction of galaxies increases with halo mass (W06). Therefore: (2) the large-scale environment surrounding a satellite galaxy will tend to be more quenched than the environment of a central of the same stellar mass. Putting (1) and (2) together, satellite contamination of the isolated primary sample creates the potential to erroneously conclude that quenched isolated primaries reside in a preferentially quenched large-scale environment, even when no signal around true centrals is present.

In this paper we use different mock galaxy catalogs, described in detail in §3 below, to investigate whether this, and other potential systematics of the K13 measurements, can result in a false signal of 2-halo conformity. The mocks we use represent realizations of different models of galaxy quenching, permitting us to directly investigate the characteristic features of halo occupation statistics that can, and cannot, give rise to the 2-halo conformity signal as measured in K13.

## 3 HALO OCCUPATION MODELS

In this section we describe the collection of halo occupation models, and their corresponding mock catalogs, that we use in our investigation of the 2-halo conformity signal. These mocks are all built by populating dark matter halos in the high-resolution Bolshoi simulation, described in §3.1. In each case, the mock galaxies are assigned stellar masses using standard (sub)halo abundance matching (SHAM) as outlined in §3.2. The models differ markedly, though, in how they connect SFRs to the mock galaxies, and so we separately review each model's approach in §3.3. For convenience, we provide a brief summary of our mocks in §3.4. We conclude this section in §3.5 by comparing the halo occupation distributions and two-point correlation functions of the mocks, explicitly demonstrating that these models give broadly similar predictions for these traditional statistics despite the radically different assumptions upon which the models are based.

### 3.1 Simulation and Halo Catalogs

The basis of the mock galaxy catalogs we construct in this paper is the collisionless N-body Bolshoi simulation (Klypin et al. 2011). The cosmological parameters of the Bolshoi run are $\Omega_m = 0.27$, $\Omega_\Lambda = 0.73$, $\Omega_b = 0.042$, $n_{\rm s} = 0.95$, $\sigma_8 = 0.82$, and $H_0 = 70$ km s$^{-1}$Mpc$^{-1}$. The simulation uses the Adaptive Refinement Tree code (ART; Kravtsov et al. 1997; Gottloeber & Klypin 2008) to solve for the evolution of $2048^3$ particles in a $250h^{-1}$Mpc periodic box. Each particle has a mass of $\mathrm{m_p} \approx 1.9 \times 10^8 h^{-1} M_\odot$; the force resolution of the simulation is $\epsilon \approx 1h^{-1}$kpc. Bolshoi snapshot data and halo catalogs are

part of the Multidark Database (Riebe et al. 2011), available at `http:www.multidark.org`.

The catalogs of dark matter halos that we use to populate our mocks are publicly available at `http://hipacc.ucsc.edu/Bolshoi/MergerTrees.html` and have been obtained using the (sub)-halo finder ROCKSTAR (Behroozi et al. 2011, 2013), which uses adaptive hierarchical refinement of friends-of-friends groups in 6 phase-space dimensions and one time dimension. Halos in these catalogs are defined to be spherical regions centered on a local density peak, such that the average density inside the sphere is $\Delta_{\rm vir} \approx 360$ times the mean matter density of the simulation box. The radius of each such sphere defines the virial radius $R_{\rm vir}$ of the halo, which is related to the mass of the halo via $M_{\rm vir} = \frac{4}{3}\pi R_{\rm vir}^3 \Delta_{\rm vir}\Omega_m \rho_{\rm crit}$, where $\rho_{\rm crit} = 3H_0^2/8\pi{\rm G}$ is the critical energy density of the universe. Subhalos in this catalog are distinct, self-bound structures that are found within the virial radius of a larger "host" halo.

### 3.2 Modeling the $\rm M_*$-Halo Connection

The first step of constructing a mock galaxy distribution is assigning galaxies with stellar mass, $M_*$, to dark matter halos or subhalos in the Bolshoi simulation. In all cases considered here, this is done using the popular SHAM technique (Kravtsov et al. 2004; Vale & Ostriker 2004; Tasitsiomi et al. 2004; Conroy et al. 2006; Shankar et al. 2006; Trujillo-Gomez et al. 2011; Rodríguez-Puebla et al. 2012; Watson et al. 2012). Abundance matching proceeds by presuming that the stellar mass of the galaxy occupying a halo increases monotonically with some (sub)halo property, $x$. For a given amount of scatter between $M_*$ and $x$, there exists a unique mapping from $x$ to $M_*$ that reproduces the observed stellar mass function. In all but one of the models studied in this paper, we use the halo property $x = {\rm V_{peak}}$, the largest value of the maximum circular velocity $\rm V_{max}$ that the halo ever attains through its entire assembly history. We refer the reader to Hearin et al. (2013) for a description of our volume-limited galaxy catalog, and Appendix A of Hearin et al. (2012) for details concerning our SHAM implementation. Additionally, we use a mock catalog kindly provided to us by Andrew Wetzel, in which the abundance matching is instead performed using $x = {\rm M_{peak}}$, the largest value of the virial mass ever attained by the halo (for details, see Wetzel et al. 2012). All mocks considered here are composed of galaxies with $M_* > 10^{9.8}{\rm M}_\odot$, and include scatter of 0.15 dex between stellar mass and the chosen halo property, in rough agreement with observational constraints (e.g., Cooray 2006; Yang et al. 2009; More et al. 2011).

We emphasize that, despite its striking simplicity, SHAM has been shown to yield a rich variety of statistics of the galaxy distribution that are in good agreement with observations, including two-point clustering over a wide range of redshifts (Conroy et al. 2006), the CLF of galaxy groups (Reddick et al. 2012), magnitude gap statistics (Hearin et al. 2012), galaxy-galaxy lensing (Hearin et al. 2013), and, indirectly, the galaxy size-stellar mass relation (Kravtsov 2013).

### 3.3 Modeling the SFR-Halo Connection

Halo occupation models can also be employed to characterize how the SFR of a galaxy is connected to the properties of its halo. Two of the models we study allow for the ability to predict the full, continuously valued SFR distribution of mock galaxies. However, in one of our models it is only possible to divide the mock galaxy sample of interest into "star-forming" and "quenched" sub-populations. To make the predictions of these models commensurable, we designate a galaxy as quenched when ${\rm sSFR} < 10^{-11}$ yr$^{-1}$. This cut is chosen to be in accord with the "persistent bimodality" of the observed SFR distribution (Wetzel et al. 2012).

#### *3.3.1 Standard HOD Model*

As mentioned in §1, in the HOD formalism, the central quantity is $P(N_{\rm gal}|M_{\rm vir})$. This quantity is typically decomposed into central and satellite contributions, accomplished by writing the first moment of $P(N_{\rm gal}|M_{\rm vir})$ as $\langle N_{\rm gal}|M_{\rm vir}\rangle = \langle N_{\rm cen}|M_{\rm vir}\rangle + \langle N_{\rm sat}|M_{\rm vir}\rangle$. It is common convention to then independently parameterize the functional forms of the central and satellite moments (see, e.g., Zheng et al. 2007, and references therein). In our SHAM-based mocks, central galaxies are galaxies that occupy distinct host halos, while satellite galaxies occupy subhalos; hence, satellite galaxies are in orbit around a central galaxy.

It is straightforward to extend this technique to further predict how quenched and star-forming subpopulations occupy dark matter halos: one simply allows the HOD parameters of star-forming and quenched populations to take on independent values (e.g., Zehavi et al. 2011). Alternatively, one may choose to model the stellar mass-dependence of galaxy occupation statistics with a standard halo model, and additionally specify the fraction of centrals and satellites in a halo of mass $M_{\rm vir}$ that are quenched, ${\rm F}_{C_{\rm Q}}(M_{\rm vir})$ and ${\rm F}_{S_{\rm Q}}(M_{\rm vir})$, respectively (see van den Bosch et al. 2003, for an early example). We adopt this second approach for the first mock catalog used in the present paper, assuming log-linear forms for the quenched fractions of satellites

$$ {\rm F}_{S_{\rm Q}}(M_{\rm vir}) = A_{\rm sat} + [\log_{10}(M_{\rm vir}) - 11]\, B_{\rm sat}\,, \qquad (1) $$

and centrals

$$ {\rm F}_{C_{\rm Q}}(M_{\rm vir}) = A_{\rm cen} + [\log_{10}(M_{\rm vir}) - 11]\, B_{\rm cen}\,. \qquad (2) $$

Here $A_{\rm x}$ and $B_{\rm x}$ are parameters of the model that in general depend on the stellar mass threshold of the galaxy sample. Note that both ${\rm F}_{S_{\rm Q}}(M_{\rm vir})$ and ${\rm F}_{C_{\rm Q}}(M_{\rm vir})$ must be bounded by zero and unity at all $M_{\rm vir}$, which we implement through the use of $\tilde{\rm F}_x$, defined as

$$ \tilde{\rm F}_x(M_{\rm vir}) \equiv {\rm MAX}\,[0, {\rm MIN}[{\rm F}_x(M_{\rm vir}), 1]]\,. \qquad (3) $$

Observations of both galaxy group statistics (Weinmann et al. 2006; Hearin et al. 2013; Watson et al. 2014) and two-point clustering (van den Bosch et al.

2003; Ross & Brunner 2009; Tinker et al. 2013) suggest that these functions increase monotonically with halo mass, so that $B_{\rm sat} > 0$ and $B_{\rm cen} > 0$.

In this formulation, the average numbers of quenched and star-forming satellite galaxies in a halo of mass $M_{\rm vir}$ are given by

$$\begin{aligned} \langle N^{\rm Q}_{\rm sat}|M_{\rm vir}\rangle &= {\rm F}_{S_{\rm Q}}(M_{\rm vir})\langle N_{\rm sat}|M_{\rm vir}\rangle \\ \langle N^{\rm SF}_{\rm sat}|M_{\rm vir}\rangle &= {\rm F}_{S_{\rm SF}}(M_{\rm vir})\langle N_{\rm sat}|M_{\rm vir}\rangle, \end{aligned} \quad (4)$$

respectively, where ${\rm F}_{S_{\rm Q}}(M_{\rm vir})+{\rm F}_{S_{\rm SF}}(M_{\rm vir}) = 1$. Directly analogous expressions apply to the corresponding occupation numbers of centrals; $\langle N^{\rm Q}_{\rm cen}|M_{\rm vir}\rangle$ and $\langle N^{\rm SF}_{\rm cen}|M_{\rm vir}\rangle$.

For the fiducial values of the parameters governing the quenched fractions in this model, we choose $A_{\rm cen} = 0.2$, $B_{\rm cen} = 0.15$, $A_{\rm sat} = 0.25$, and $B_{\rm sat} = 0.15$. These fiducial values were chosen based on the corresponding values predicted by the age matching model, described below in §3.3.3. Since the age matching model has already been shown to make highly realistic predictions for the galaxy distribution observed in SDSS, tuning our HOD parameters to resemble the age matching model's ensures that the resulting mock is realistic in turn. However, we stress that all of our conclusions regarding 2-halo conformity are insensitive to this choice.

Once a set of fiducial values are chosen for the HOD parameters, it is straightforward to construct a mock galaxy catalog that serves as a realization of the model. As described in §3.2, we begin with abundance matching to create a sample of mock centrals and satellites. Next we assign each galaxy as either 'quenched' or 'star forming' using simple Monte Carlo techniques, where we interpret ${\rm F}_{C_{\rm Q}}(M_{\rm vir})$ and ${\rm F}_{S_{\rm Q}}(M_{\rm vir})$ as the probabilities that a central or satellite galaxy is quenched.

#### *3.3.2 Delayed-Then-Rapid Model*

The SFR designation in the second mock catalog comes from the "delayed-then-rapid" quenching model introduced in Wetzel et al. (2012), to which we refer the reader for details. Briefly, a mock central galaxy with stellar mass $M_*$ is assigned an SFR value by randomly selecting an SDSS central galaxy with a similar $M_*$, where the group finding algorithm introduced in Tinker et al. (2011) is used to identify SDSS centrals. Because abundance matching was used to assign the value of $M_*$ to host halos in this catalog, this model effectively assumes that central galaxy quenching statistics are governed by $M_{\rm vir}$ alone.

For satellite galaxies, which are associated with present-day subhalos, special physical significance is attached to $t_{\rm acc}$, the epoch the subhalo first passes within the virial radius of some other, more massive host halo. Prior to $t_{\rm acc}$, satellite galaxies are presumed to have evolved as centrals. Using a model for how the SFR distribution of central galaxies scales with redshift, each present-day satellite galaxy is first assigned a SFR at time $t_{\rm acc}$ that is appropriate for its stellar mass at that epoch. If at accretion the satellite is already quenched, it is assumed to remain quenched. Otherwise, its SFR is assumed to undergo exponential quenching, on an e-folding time scale of $\tau_{\rm Q} = \tau_{\rm Q}(M_*) \simeq 0.2-0.8$Gyr, but only after a delay-time of $t_{\rm delay} = t_{\rm delay}(M_*) \simeq 2-4$Gyr. The stellar mass dependencies of $\tau_{\rm Q}(M_*)$ and $t_{\rm delay}(M_*)$ have been tuned to match the quenched fractions and quenching gradients of satellite galaxies in the Tinker et al. (2011) SDSS group catalog. Thus the SFRs of satellites in this model are determined by both halo mass *at* accretion, ${\rm M}_{\rm acc}$, and by the time *since* accretion, $t - t_{\rm acc}$.

As shown in Wetzel et al. (2014), a significant subpopulation of present day host halos is comprised of "ejected" (or "backsplash") galaxies, which are halos that have previously been identified as subhalos at some point in their assembly history. These objects are modeled in an identical fashion as the satellites associated with present-day subhalos, so that ejected satellites quench exponentially at a time $t_{\rm delay}$ after they first passed within a distance $R_{\rm vir}$ of some larger halo. As shown in Wetzel et al. (2014), treating backsplash galaxies on par with satellite galaxies provides an explanation for the enhanced SFR quenching observed out to $\sim 2.5R_{\rm vir}$ for groups and clusters. However, as we show below, backsplashing is not sufficient to explain the 2-halo conformity observed by K13.

#### *3.3.3 Age Matching Model*

The third mock catalog used in this paper is generated with the age matching technique. The formalism was introduced in Hearin & Watson (2013) and extended in Hearin et al. (2013), and was shown to predict a variety of SDSS galaxy statistics as a function of $g-r$ color. It was recently generalized to predict SFRs in Watson et al. (2014). In age matching, no explicit distinction is made between centrals and satellites, and no special significance is attached to $R_{\rm vir}$. At fixed stellar mass, SFR values are randomly drawn from the distribution of SDSS galaxies with the corresponding $M_*$. The lowest SFR values are assigned to the "oldest" (sub)halos, where (sub)halo age is quantified by the halo property $z_{\rm starve}$, which is primarily determined by the epoch in the very distant past where the (sub)halo transitioned from the fast- to slow-mass accretion regime (Wechsler et al. 2002; Zhao et al. 2003). Thus in age matching, galaxy assembly bias of both centrals and satellites is quite strong, since at fixed $M_*$ galaxy SFR is in monotonic correspondence with a marker of halo assembly time (see Zentner et al. 2013).

### 3.4 Summary of Mocks

**Mock 1:** *Standard HOD model.* Quenching of both centrals and satellites depends only on $M_{\rm vir}$.

**Mock 2:** *Delayed-then-rapid model.* Quenching of centrals depends only on $M_{\rm vir}$. Quenching of satellites and backsplash galaxies depends on both ${\rm M}_{\rm acc}$ and $(t - t_{\rm acc})$.

**Mock 3:** *Age matching model.* Quenching of centrals and satellites depends on both $M_{\rm vir}$ and (sub)halo formation time.

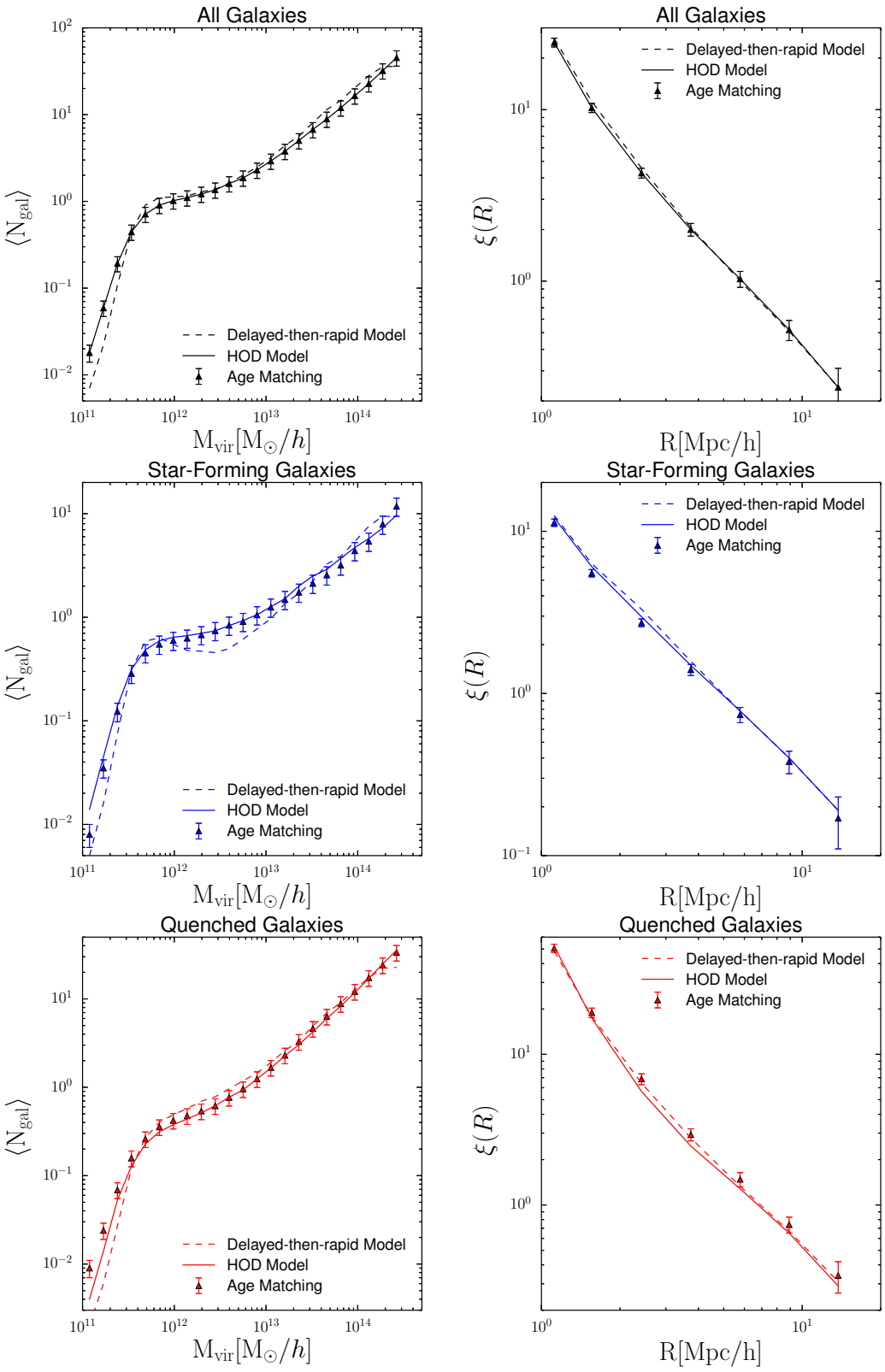


**Figure 1. Comparison of our three quenching models.** The *left* column of panels shows the mean number of galaxies occupying halos of a given mass $M_{\rm vir}$. Two-point correlation functions appear in the *right* panels, plotted as a function of 3D separation. The top panels refer to the full, volume-limited mock galaxy samples (with stellar mass thresholds $M_* > 10^{9.8}{\rm M}_\odot$) in each mock, the middle and bottom panels show the star-forming and quenched subpopulations, respectively. The broad agreement between these galaxy distributions is striking given how radically these models differ from one another in their predictions for the processes that govern quenching. See §5.2 for further discussion.

### 3.5 Model Comparison

We conclude this section by comparing some statistics of the three mocks introduced above. For mock galaxies with $M_* > 10^{9.8}\mathrm{M}_\odot$, Fig. 1 shows the HODs, $\langle N_{\rm gal}|M_{\rm vir}\rangle$, in the left-hand panels, and two-point correlation functions, $\xi(r)$, in the right-hand panels. Results are shown for all galaxies (upper panels), star-forming galaxies (middle panels), and quenched galaxies (lower panels).

All three mocks have, by construction, the same stellar mass function, but differ in the way the mock galaxies were split into quenched and star forming subpopulations. Although none of the mocks has been tuned to reproduce the observed clustering, or to agree with the clustering of any of the other mocks, they have halo occupation statistics and clustering properties that are remarkably similar. This indicates that both of these one- and two-point functions, which are commonly used to quantify halo occupation statistics, are largely insensitive to the differences between these three mock galaxy distributions. This is despite the fact that they represent radically different perspectives on the physical processes that drive galaxy quenching. These results are especially noteworthy because, as we will see, 2-halo conformity brings the differences between these models into sharp relief.

## 4 MOCK OBSERVATIONS OF 2-HALO CONFORMITY

We now proceed to apply the K13 methodology to our mocks in order to investigate whether they reveal any sign of 2-halo conformity. We begin by identifying isolated primary galaxies in the mocks using the K13 criteria. In particular, we place the mock galaxies into redshift-space by invoking the distant observer approximation, using the simulation's z-axis as the line-of-sight. A galaxy with stellar mass $M_*$ is labeled as an isolated primary if a cylinder with a line-of-sight length of $\pm$500 km/s and radius of 500 kpc/h contains no other mock galaxies with stellar mass greater than $M_*/2$.

We deviate from K13 in that we measure 2-halo conformity using the mean quenched fractions, rather than $\langle$SFR$\rangle$. As discussed in §3.3, this choice is made to simultaneously accommodate all three of our mocks. In addition, whereas K13 measured 2-halo conformity in projection, and presented the signal as a function of the radius of the cylindrical annulus centered on the isolated primary, we present our measurements of 2-halo conformity as a function of the 3D distance from the isolated primary. Since the salient point of this paper is that halo occupation models without central galaxy assembly bias contain no statistically significant level of 2-halo conformity, it suffices to demonstrate that this fact holds true when the signal is measured in the 3D galaxy distribution. After all, projection effects will only diminish the true signal strength. Finally, for brevity, we only focus on the stellar mass range $10^{10}\mathrm{M}_\odot < M_* < 10^{10.5}\mathrm{M}_\odot$ of primaries, which corresponds to the lower end of the range studied in K13, for which the observed signal is strongest. In the Appendix, we investigate how the signal varies with the stellar mass of the primary, and in

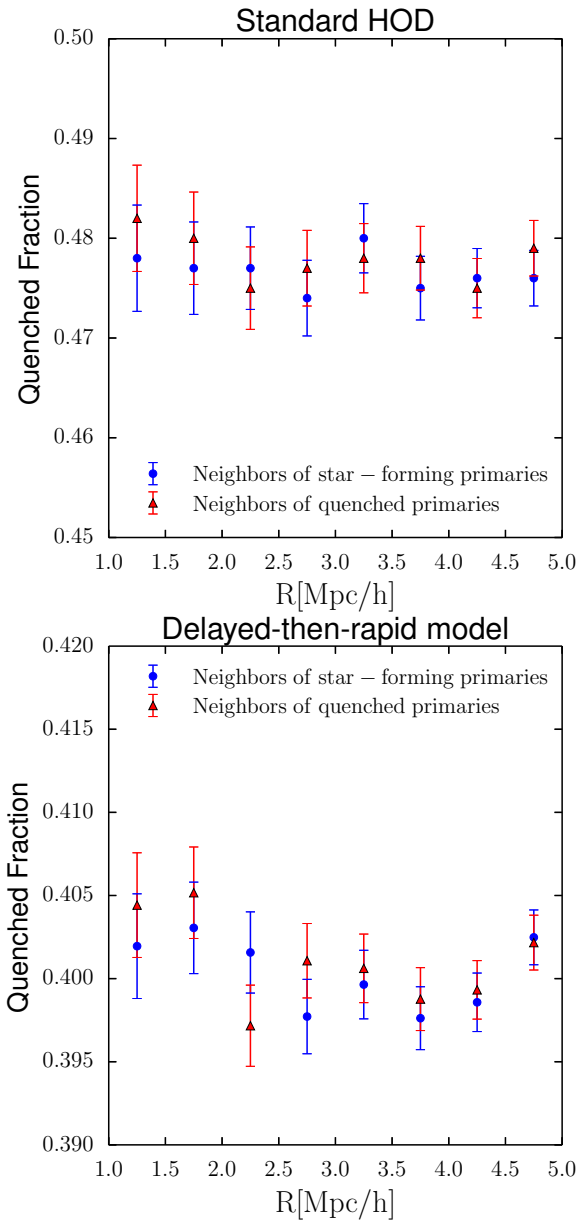


**Figure 2.** In each panel, the vertical axis shows the mean quenched fraction of all galaxies neighboring samples of "isolated primaries" selected in the same manner as in Kauffmann et al. (2013). Horizontal axes are the 3D distance from the primary. The *top* panel shows the 2-halo conformity signal around isolated primaries with $10^{10}\mathrm{M}_\odot < M_* < 10^{10.5}\mathrm{M}_\odot$ as predicted by the standard HOD quenching model described in §3.3.1. Standard HOD models predict that the SFR of galaxies occupying distinct halos are uncorrelated, giving rise to zero 2-halo conformity, in contrast to the relatively strong signal measured in K13 (see their Figs. 2 & 3). The *bottom* panel is the same as the top panel, only here we show the prediction of the "delayed-then-rapid" model described in §3.3.2. There is little-to-no signal, again in contrast with the K13 measurements. This demonstrates that satellite backsplashing alone cannot account for the observed level of 2-halo conformity, and furthermore implies that the role of post-infall processes on satellite quenching has been overestimated in this and related models. See §4.2 and §5.3 for further discussion.

so doing we rule out a still broader class of HOD models than the one introduced in §3.3.1. A more thorough exploration of the $M_*$-dependence of 2-halo conformity will be presented in Paper III.

### 4.1 Standard HOD Predictions of 2-Halo Conformity

As a first test, we consider the standard HOD mock described in §3.3.1. For each isolated primary, identified using the method described in § 4, we compute the quenched fraction of all neighboring galaxies in spherical shells centered on the primary. The upper panel of Fig. 2 shows the mean quenched fraction as a function of the 3D distance from the primary. Red and blue symbols correspond to the mean quenched fractions around quenched and star-forming isolated primaries, respectively, while the error bars reflect the uncertainties assuming Poisson statistics.

The fact that the red and blue points are consistent with each other within the errors indicates that this mock does not reveal any significant 2-halo conformity over the range 1Mpc/h $\lesssim R \lesssim$ 5Mpc/h. This may not come as a surprise given that this mock, by construction, does not have any 2-halo conformity built in. However, this serves to demonstrate that satellite contamination, as described in §2.2, does not introduce an artificial signal of 2-halo conformity. The fraction of isolated primaries that are contaminating satellites, as opposed to true centrals, is only a few percent. As is clear from the upper panel in Fig. 2, this minor level of contamination has no detectable influence on the measured 2-halo conformity signal.

By constructing similar HOD mocks, but using different combinations of quenching parameters $\mathrm{A}_x$ and $\mathrm{B}_x$ (see Eqs. 1-2), we find that the lack of 2-halo conformity on scales $R \gtrsim 1$ Mpc/h is robust to the particular form of the quenching functions $\mathrm{F}_{S_\mathrm{Q}}(M_\mathrm{vir})$ and $\mathrm{F}_{C_\mathrm{Q}}(M_\mathrm{vir})$. Hence, we conclude that satellite contamination in the K13 measurements is unlikely to have introduced a false signal of 2-halo conformity, and that the results of K13 are inconsistent with models in which the quenching statistics of galaxies are solely regulated by halo mass $M_\mathrm{vir}$.

### 4.2 2-Halo Conformity and Satellite Backsplashing

The conclusions drawn at the end of the last section raise the following natural question: is it possible for 2-halo conformity to be predicted by a model in which deviations from $M_\mathrm{vir}$-determined occupation statistics are limited to satellite galaxies? Or must beyond-$M_\mathrm{vir}$ effects be present in central galaxies in order to give rise to the signal measured in K13?

The delayed-then-rapid mock is an ideal testing ground for this purpose, because, as discussed in §3.3.2, galaxy assembly bias in this model is limited to satellites (including the population of backsplash galaxies). Moreover, in this model even the quenching of satellites is strongly influenced by (sub)halo mass: since satellites are presumed to evolve as centrals prior to $t_\mathrm{acc}$, a satellite's "initial" SFR is essentially set by the mass of its host halo at the time of infall, $\mathrm{M_{acc}}$ . In this sense, this model provides a kind of minimal extension to standard halo occupation modeling of galaxy quenching.

It is at least plausible that the treatment of satellite backsplashing in the delayed-then-rapid model leads to some non-zero level of 2-halo conformity. As shown in Wetzel et al. (2014), $\sim 10\%$ of the population of present-day $M_* \sim 10^{10}\mathrm{M}_\odot$ centrals are actually ejected satellites residing outside the virial radius of massive halos. These galaxies will tend to gather near each other through their common association with a massive host, and they will also tend to be quenched. Thus if a large enough fraction of these backsplashed satellites pass the K13 isolation criteria, it is possible that the SFR correlations amongst backsplashed satellites could produce a 2-halo conformity signal.

We directly test this possibility in the bottom panel of Fig. 2, which is the same as the top panel but for the delayed-then-rapid mock. The bottom panel shows that satellite backsplashing has a negligible effect on 2-halo conformity on scales 1Mpc/h $\lesssim R \lesssim$ 5Mpc/h. Recall that the conformity signal shown in Fig. 2, as with all figures in this paper, is computed in 3D to identify the true strength of the signal.

The bottom panel of Fig. 2 rules out the possibility that satellite backsplashing alone can explain the strength of the signal reported in K13. Given the other successful, quantitative predictions of this model, this is an interesting observation in and of itself since it suggests that 2-halo conformity contains information about galaxy evolution that is independent from more traditional statistics (see §5.2 for further discussion of this point). More importantly, the failure of this mechanism to predict 2-halo conformity is highly suggestive of the conclusion that galaxy assembly bias in centrals, not just satellites, is responsible for the observed level of 2-halo conformity. We investigate this possibility with the age matching mock in the following section.

### 4.3 2-Halo Conformity and Central Galaxy Assembly Bias

We now turn to the age matching mock, in which the prescription for assigning SFRs to mock galaxies is predicated on the assumption that galaxies co-evolve with their dark matter halos (see §3.3.3). The top panel of Fig. 3 shows that, contrary to the previous two mocks discussed above, age matching results in a highly significant 2-halo conformity signal. The quenched fraction of neighboring galaxies is much larger around quenched primaries than around star-forming primaries. We emphasize that this result is obtained without any modification to the age matching technique introduced in the recent trilogy of papers describing this model (Hearin & Watson 2013; Hearin et al. 2013; Watson et al. 2014).

It is easy to understand why age matching gives rise to 2-halo conformity: halos that collapse from the same region of the cosmic density field have correlated assembly histories. In age matching, the stellar mass assembly

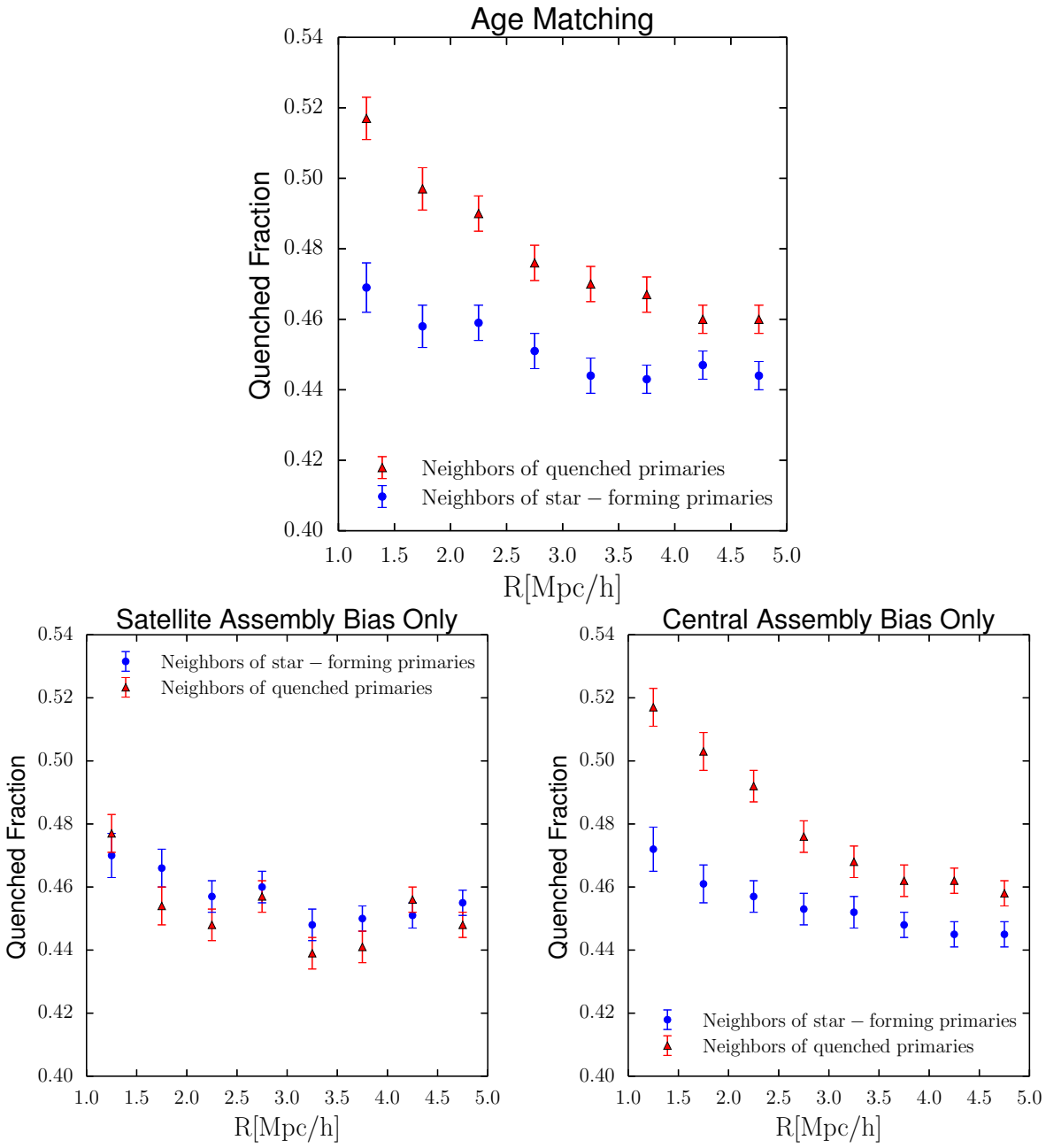


**Figure 3. Age Matching prediction of 2-halo conformity.** All panels are the same as in Fig. 2, only here the age matching model is used to investigate the relationship between galaxy assembly bias and 2-halo conformity. The *top* panel shows the 2-halo conformity prediction of age matching, in which galaxy assembly bias in both centrals and satellites is quite strong. For the model shown in the *bottom left* panel, we have scrambled the SFRs of central galaxies residing in halos of similar mass $M_{\rm vir}$, which erases the strong signal shown in the top panel. In the *bottom right* panel, we have instead scrambled the SFRs of satellite galaxies, which only marginally influences the 2-halo conformity signal. Together with Fig. 2, these results provide strong support for the conclusion that the level of 2-halo conformity measured in K13 is driven by *central* galaxy assembly bias (see §5.1 for further discussion).

history of a galaxy is directly tied to the mass assembly history of the galaxy's parent (sub)halo. Therefore a natural feature of age matching is that the SFRs of galaxies in the same large-scale environment are correlated, regardless of whether the galaxies occupy distinct dark matter halos.

In light of the discussion and results in §4.2, a natural question to ask is whether the conformity signal in age matching is driven by central galaxies or satellites. In fact there are many "beyond $M_{\rm vir}$" phenomena predicted by age matching, including both intra-halo effects and also large-scale effects exhibited by both central and

satellite galaxies.[3] Thus it is not clear from the top panel of Fig. 3 alone whether the 2-halo conformity signal predicted by age matching is due to galaxy assembly bias in the centrals, satellites, or both.

Fortunately, the following shuffling exercises make it straightforward to identify the source of the signal in age matching. For the model plotted in the bottom left panel of Fig. 3, we start with the age matching mock and scramble the SFR designation of *central* galaxies that reside in halos of similar mass. Operationally, we bin the centrals by the value of $M_{\rm vir}$ of their host halo, using bin widths of 0.1 dex, and randomly shuffle the SFR designations amongst the centrals in that bin. We then recompute the 2-halo conformity signal around isolated primaries with stellar mass $10^{10}{\rm M}_{\odot} < M_{*} < 10^{10.5}{\rm M}_{\odot}$, and show the result in the bottom-left panel of Fig. 3. Interestingly, this scrambling entirely erases the 2-halo conformity signal in the mock, suggesting that central galaxies are responsible for the signal. The bottom-right panel is the same as the bottom left, but this time we have performed the shuffling exercise with the SFR designations of the *satellites*, leaving the central SFRs fixed to their age matching-predicted values. The effect of this satellite scrambling is very different: in this case, the 2-halo conformity signal is left unadulterated. These shuffling exercises imply that the strong 2-halo conformity signal predicted by age matching is almost entirely due to the model's treatment of central galaxies.

To be clear, the purpose of Figure 3 is not to claim that age matching is the "correct" or only model of 2-halo conformity. Rather, *the role of the age matching model in this paper is merely to provide an illustrative example of a galaxy-halo model in which the signal is strong.* This is valuable, because the top panel of Fig. 2 makes it highly implausible that a standard HOD model can predict the signal, while the bottom panel of Fig. 2 shows that one of the leading empirical models of satellite quenching predicts virtually no signal. In addition, K13 has shown that the state-of-the-art SAM of Guo et al. (2011) predicts little to no 2-halo conformity signal either. Fig. 3 serves to demonstrate that levels of 2-halo conformity as strong as the K13 measurements do not require any "spooky action-at-a-distance", nor detailed modeling of complex astrophysical phenomena. If the star formation history of central galaxies traces the mass assembly history of host halos in some manner similar to age matching, 2-halo conformity emerges naturally.

## 5 DISCUSSION & OUTLOOK

### 5.1 2-Halo Conformity as an Assembly Bias Marker

The results in §4 support the conclusion that the K13 measurements of 2-halo conformity constitute a detection of *central galaxy assembly bias.* We use this term to mean that central galaxy SFR is significantly correlated with some halo property in addition to halo mass $M_{\rm vir}$. The evidence for this conclusion is straightforward.

First, in the top panel of Fig. 2, we have shown that standard HOD models of galaxy quenching, in which there is no assembly bias of any kind, predict that 2-halo conformity should be zero in the stellar mass range where it has been observed with high statistical significance ($10^{10}{\rm M}_{\odot} < M_{*} < 10^{10.5}{\rm M}_{\odot}$). Although Fig. 2 only shows that this is the case for a particular choice of HOD parameters, we find that this conclusion holds regardless of the fiducial values of the parameters. The K13 signal is not easily computable within the analytical framework of the halo model, necessitating this mock catalog-based approach.

Second, we have shown that 2-halo conformity is also zero in two very different quenching models in which the galaxy assembly bias is limited to satellites. The first is the delayed-then-rapid model put forth in Wetzel et al. (2012), and shown in the bottom panel of Fig. 2. In the second case, we consider an alteration to the age matching model (Hearin & Watson 2013) wherein we scramble the SFRs of *central* galaxies, at fixed halo mass. Both of these models produce essentially zero 2-halo conformity for scales $1{\rm Mpc/h} \lesssim R \lesssim 5{\rm Mpc/h}$. However, when we then test a mock in which *satellite* galaxy SFRs have been scrambled in the age matching model (bottom right panel of Fig. 3), the signal is nearly as strong as it is in the unscrambled age matching mock (top panel of Fig. 3). This directly implies that central galaxy assembly bias is responsible for the 2-halo conformity signal predicted by this model.

Although we acknowledge that these results do not conclusively rule out a relationship between 2-halo conformity and satellite SFR, simply because our exploration of satellite-based models has been far from exhaustive, the fact that centrals dominate the abundance of galaxies at all stellar masses of interest clearly supports the notion that any 2-halo conformity is likely to be driven by central galaxies rather than satellites.

Detections of central galaxy assembly bias have been reported in a growing body of literature. For example, numerous studies of SDSS galaxy samples (e.g., Yang et al. 2005, 2006; Wang et al. 2008, 2013) have employed galaxy group finders to demonstrate that the clustering of central galaxies (or the clustering of the groups themselves) depends on star formation indicators even after controlling for halo mass. The results presented in §2 complement these previously reported detections with a method that has no reliance on a group-finding algorithm: both the K13 measurements and the above group-finder based methods support the notion that the statistics describing the quenching of galaxies are not solely a function of halo mass $M_{\rm vir}$ alone.

### 5.2 2-Halo Conformity as a New Probe of Galaxy Evolution

The delayed-then-rapid model presented in Wetzel et al. (2012) attaches unique physical significance to the virial radius $R_{\rm vir}$ of the dark matter halo: central galaxy quenching statistics are exclusively governed by the mass

[3] See Zentner et al. (2013) for an extensive study of the character of assembly bias predicted by age matching.

$M_{\rm vir}$ enclosed by the virial radius, and the SFR of satellites only begins to differ from centrals some time after $t_{\rm acc}$, when the satellite first passes within $R_{\rm vir}$ of a larger halo. This model can be tuned to accurately reproduce a number of well-studied statistics based on galaxy group catalogs, such as the quenched fraction of satellites as a function of group mass, and the radial quenching gradients of satellites (Wetzel et al. 2014). Moreover, we have shown in Fig. 1 that the two-point correlation functions predicted by this model are in close agreement with the predictions of the age matching model, which itself accurately fits data from the SDSS (Hearin & Watson 2013; Hearin et al. 2013; Watson et al. 2014). Hence, we conclude that the shortcomings of the delayed-then-rapid model are not revealed by conventional statistics, but only become apparent when using the 2-halo conformity signal. This demonstrates that this new statistic possesses heretofore untapped constraining power for models of galaxy evolution.[4]

Another example supporting the notion that the information content of 2-halo conformity is largely independent from that of more traditional statistics is the SAM presented in Guo et al. (2011). This model reproduces reasonably well the observed clustering of galaxies as a function of stellar mass and color, as well as the distribution of galaxies within rich clusters. And yet, as shown explicitly in K13, this model predicts little-to-no 2-halo conformity. In K13, the authors speculate that 2-halo conformity may arise under a modification to the Guo et al. SAM in which there is "pre-heating" of the inter-galactic medium (IGM) at early times. This possibility is intriguing in light of the recent results presented in Lu et al. (2014), who showed that pre-heating of the IGM may play an important role in establishing numerous scaling relations of disk galaxies.

### 5.3 Toward a New Picture of Satellite Quenching

The significant levels of 2-halo conformity measured in K13 suggest a different picture of galaxy evolution than the one offered by the prevailing paradigm. In particular, this signal indicates that contemporary models of satellite quenching have systematically over-estimated the significance of post-infall physical processes on attenuating the SFRs of satellite galaxies. This conclusion derives from the following chain of reasoning.

First, the results of this work together with the K13 measurements strongly suggest that the large-scale environment ($R \sim 1-5$ Mpc) of a central galaxy is correlated, *at fixed* $M_{\rm vir}$, with processes influencing the star formation history of the central. And so if satellites evolve as centrals for most of cosmic time, just as subhalos lead most of their lives as host halos, then these same processes should also be at work in quenching the satellites.[5]

Second, at fixed $M_*$, galaxies that end up as satellites are far more likely to evolve in a dense large-scale environment. Therefore, the quenching mechanisms that correlate with large scale environment at fixed $M_{\rm vir}$ will have had a statistically greater influence on the present-day satellite population, which will tend to produce preferentially quenched satellites *even in the complete absence of post-infall specific processes*. Models of galaxy quenching that ignore the above fact about structure growth in CDM are left with little choice but to rely too heavily on post-infall processes in order to reproduce the observed excess quenched fractions of satellites relative to centrals of the same $M_*$. We conclude that careful comparisons to 2-halo conformity measurements (and other unambiguous markers of galaxy assembly bias) should henceforth be considered an essential component of modeling and constraining the star formation histories of galaxies.

[4] See also Cohn & White (2014) for an extensive investigation of the information content contained in alternative statistics to two-point clustering at $z \sim 0.5$.

[5] See Watson & Conroy (2013) for further empirical justification of the notion that satellites do indeed evolve as centrals for most of cosmic history.

## ACKNOWLEDGEMENTS

APH is supported by the U.S. Department of Energy under contract No. DE-AC02-07CH11359, and by a fellowship provided by the Yale Center for Astronomy & Astrophysics. DFW is supported by the National Science Foundation under Award No. AST-1202698. Our thanks to Alyson Brooks, Matt Becker, Risa Wechsler, Michael Busha, Yu Lu, Duncan Campbell, and Andrew Zentner for useful discussions. Special thanks are due to Andrew Wetzel for sharing his mock catalog, and to Andrew Wetzel, Charlie Conroy, and Jeremy Tinker for extensive comments on an early draft. We thank The Sound Defects for *Iron Horse.*

## REFERENCES

Abazajian K. N., Adelman-McCarthy J. K., Agüeros M. A., Allam S. S., Allende Prieto C., An D., Anderson K. S. J., Anderson S. F., Annis J., Bahcall N. A., et al. 2009, ApJS , 182, 543

Behroozi P. S., Wechsler R. H., Wu H.-Y., 2011, ArXiv:1110.4372

Behroozi P. S., Wechsler R. H., Wu H.-Y., Busha M. T., Klypin A. A., Primack J. R., 2013, ApJ , 763, 18

Berlind A. A., Weinberg D. H., 2002, ApJ , 575, 587

Blanton M. R., Schlegel D. J., Strauss M. A., Brinkmann J., Finkbeiner D., Fukugita M., Gunn J. E., Hogg D. W., Ivezić Ž., Knapp G. R., Lupton R. H., Munn J. A., Schneider D. P., Tegmark M., Zehavi I., 2005, AJ , 129, 2562

Cacciato M., van den Bosch F. C., More S., Mo H., Yang X., 2013, MNRAS , 430, 767

Cohn J. D., White M., 2014, MNRAS

Collister A. A., Lahav O., 2005, MNRAS , 361, 415

Conroy C., Wechsler R. H., Kravtsov A. V., 2006, ApJ , 647, 201

Cooray A., 2006, MNRAS , 365, 842

Cooray A., Sheth R., 2002, Phys. Rep. , 372, 1

Dalal N., White M., Bond J. R., Shirokov A., 2008, ApJ , 687, 12
Gao L., Springel V., White S. D. M., 2005, MNRAS , 363, L66
Gao L., White S. D. M., 2007, MNRAS , 377, L5
Gottloeber S., Klypin A., 2008, ArXiv:0803.4343
Guo H., Zheng Z., Zehavi I., Xu H., Eisenstein D. J., Weinberg D. H., Bahcall N. A., Berlind A. A., Comparat J., McBride C. K., Ross A. J., Schneider D. P., Skibba R. A., Swanson M. E. C., Tinker J. L., Tojeiro R., Wake D. A., 2014, ArXiv:1401.3009
Guo Q., White S., Boylan-Kolchin M., De Lucia G., Kauffmann G., Lemson G., Li C., Springel V., Weinmann S., 2011, MNRAS , 413, 101
Hearin A. P., Watson D. F., 2013, ArXiv:1304.5557
Hearin A. P., Watson D. F., Becker M. R., Reyes R., Berlind A. A., Zentner A. R., 2013, ArXiv:1310.6747
Hearin A. P., Zentner A. R., Berlind A. A., Newman J. A., 2012, ArXiv:1210.4927
Kauffmann G., Li C., Zhang W., Weinmann S., 2013, MNRAS , 430, 1447
Klypin A. A., Trujillo-Gomez S., Primack J., 2011, ApJ , 740, 102
Kravtsov A. V., 2013, ApJL , 764, L31
Kravtsov A. V., Berlind A. A., Wechsler R. H., Klypin A. A., Gottlöber S., Allgood B., Primack J. R., 2004, ApJ , 609, 35
Kravtsov A. V., Klypin A. A., Khokhlov A. M., 1997, ApJS , 111, 73
Lacerna I., Padilla N., 2011, MNRAS , 412, 1283
Lacerna I., Padilla N., 2012, MNRAS , 426, L26
Leauthaud A., et al., 2011, ArXiv:1104.0928
Li Y., Mo H. J., Gao L., 2008, MNRAS , 389, 1419
Lu Y., Mo H. J., Wechsler R. H., 2014, ArXiv:1402.2036
Magliocchetti M., Porciani C., 2003, MNRAS , 346, 186
Mandelbaum R., Seljak U., Kauffmann G., Hirata C. M., Brinkmann J., 2006, MNRAS , 368, 715
Mo H., van den Bosch F. C., White S., 2010, Galaxy Formation and Evolution. Cambridge University Press, Cambridge, UK
Mo H. J., Mao S., White S. D. M., 1998, MNRAS , 295, 319
Mo H. J., White S. D. M., 1996, MNRAS , 282, 347
More S., van den Bosch F. C., Cacciato M., More A., Mo H., Yang X., 2013, MNRAS , 430, 747
More S., van den Bosch F. C., Cacciato M., Skibba R., Mo H. J., Yang X., 2011, MNRAS, 410, 210
Phillips J. I., Wheeler C., Boylan-Kolchin M., Bullock J. S., Cooper M. C., Tollerud E. J., 2014, MNRAS , 437, 1930
Reddick R. M., Wechsler R. H., Tinker J. L., Behroozi P. S., 2012, ArXiv:1207.2160
Riebe K., Partl A. M., Enke H., Forero-Romero J., Gottloeber S., Klypin A., Lemson G., Prada F., Primack J. R., Steinmetz M., Turchaninov V., 2011, ArXiv:1109.0003
Rodríguez-Puebla A., Drory N., Avila-Reese V., 2012, ApJ , 756, 2
Ross A. J., Brunner R. J., 2009, MNRAS , 399, 878
Ross A. J., Percival W. J., Brunner R. J., 2010, MNRAS , 407, 420
Seljak U., 2000, MNRAS , 318, 203
Shankar F., Lapi A., Salucci P., De Zotti G., Danese L., 2006, ApJ , 643, 14
Simon P., Hetterscheidt M., Wolf C., Meisenheimer K., Hildebrandt H., Schneider P., Schirmer M., Erben T., 2009, MNRAS , 398, 807
Skibba R. A., Sheth R. K., 2009, MNRAS , 392, 1080
Tasitsiomi A., Kravtsov A. V., Wechsler R. H., Primack J. R., 2004, ApJ , 614, 533
Tinker J., Wetzel A., Conroy C., 2011, ArXiv:1107.5046
Tinker J. L., Leauthaud A., Bundy K., George M. R., Behroozi P., Massey R., Rhodes J., Wechsler R., 2013, ArXiv:1308.2974
Tinker J. L., Weinberg D. H., Zheng Z., Zehavi I., 2005, ApJ , 631, 41
Trujillo-Gomez S., Klypin A., Primack J., Romanowsky A. J., 2011, ApJ , 742, 16
Vale A., Ostriker J. P., 2004, MNRAS , 353, 189
van den Bosch F. C., Aquino D., Yang X., Mo H. J., Pasquali A., McIntosh D. H., Weinmann S. M., Kang X., 2008, MNRAS , 387, 79
van den Bosch F. C., Mo H. J., Yang X., 2003, MNRAS , 345, 923
van den Bosch F. C., More S., Cacciato M., Mo H., Yang X., 2013, MNRAS , 430, 725
van den Bosch F. C., Yang X., Mo H. J., 2003, MNRAS , 340, 771
van den Bosch F. C., Yang X., Mo H. J., Weinmann S. M., Macciò A. V., More S., Cacciato M., Skibba R., Kang X., 2007, MNRAS , 376, 841
Wang L., Weinmann S. M., De Lucia G., Yang X., 2013, MNRAS , 433, 515
Wang Y., Yang X., Mo H. J., van den Bosch F. C., Weinmann S. M., Chu Y., 2008, ApJ , 687, 919
Watson D. F., Berlind A. A., Zentner A. R., 2011, ApJ , 738, 22
Watson D. F., Berlind A. A., Zentner A. R., 2012, ApJ , 754, 90
Watson D. F., Conroy C., 2013, ApJ , 772, 139
Watson D. F., Hearin A. P., Berlind A. A., Becker M. R., Behroozi P. S., Skibba R. A., Reyes R., Zentner A. R., 2014, ArXiv:1403.1578
Wechsler R. H., Bullock J. S., Primack J. R., Kravtsov A. V., Dekel A., 2002, ApJ , 568, 52
Wechsler R. H., Zentner A. R., Bullock J. S., Kravtsov A. V., Allgood B., 2006, ApJ , 652, 71
Weinmann S. M., van den Bosch F. C., Yang X., Mo H. J., 2006, MNRAS , 366, 2
Wetzel A. R., Cohn J. D., White M., Holz D. E., Warren M. S., 2007, ApJ , 656, 139
Wetzel A. R., Tinker J. L., Conroy C., 2012, MNRAS , 424, 232
Wetzel A. R., Tinker J. L., Conroy C., Bosch F. C. v. d., 2014, MNRAS , 439, 2687
Yang X., Mo H. J., van den Bosch F. C., 2003, MNRAS , 339, 1057
Yang X., Mo H. J., van den Bosch F. C., 2006, ApJL , 638, L55
Yang X., Mo H. J., van den Bosch F. C., 2008, ApJ , 676, 248
Yang X., Mo H. J., van den Bosch F. C., 2009, ApJ , 695, 900

Yang X., Mo H. J., van den Bosch F. C., Weinmann S. M., Li C., Jing Y. P., 2005, MNRAS , 362, 711
York D. G., et al., 2000, AJ , 120, 1579
Zehavi I., et al., 2005, ApJ , 630, 1
Zehavi I., et al., 2011, ApJ , 736, 59
Zentner A. R., Hearin A. P., van den Bosch F. C., 2013, ArXiv:1311.1818
Zhao D. H., Mo H. J., Jing Y. P., Börner G., 2003, MNRAS , 339, 12
Zheng Z., Berlind A. A., Weinberg D. H., Benson A. J., Baugh C. M., Cole S., Davé R., Frenk C. S., Katz N., Lacey C. G., 2005, ApJ , 633, 791
Zheng Z., Coil A. L., Zehavi I., 2007, ApJ , 667, 760
Zheng Z., Zehavi I., Eisenstein D. J., Weinberg D. H., Jing Y. P., 2009, ApJ , 707, 554

## APPENDIX A: THE (IN)SIGNIFICANCE OF DISTINCT $M_* - M_{\rm vir}$ RELATIONS FOR STAR-FORMING AND QUENCHED CENTRALS

As discussed in §4.1, our standard HOD mock does not reveal any significant 2-halo conformity, indicating that satellite contamination is not a major concern. It also suggests that 2-halo conformity is inconsistent with the standard "$M_{\rm vir}$-only" paradigm for halo occupation statistics. However, the HOD model that we considered implicitly assumes that the $M_* - M_{\rm h}$ relation is the same for quenched and star-forming centrals. Yet, results deriving from the analysis of satellite kinematics indicate that this assumption may be violated, and that the average halo mass of star-forming central galaxies may be distinct from that of quenched centrals (More et al. 2011). This is also supported by HOD analyses of two-point clustering and galaxy-galaxy lensing (Mandelbaum et al. 2006; Tinker et al. 2013). Naively, this indicates that the range of models spanned by the quenching formulation presented in §3.3.1 may not be general enough to rule out "$M_{\rm vir}$-only" models of galaxy quenching statistics.

In fact, different $M_* - M_{\rm h}$ relations for star-forming and quenched centrals could potentially produce a 2-halo conformity signal. Suppose that quenched centrals reside, on average, in more massive halos than star-forming centrals of the same stellar mass. Since halo clustering strength increases with halo mass, quenched centrals will find themselves surrounded by more massive halos than star-forming centrals. And because the quenched fraction increases with halo mass for centrals and satellites alike, the environment of quenched centrals will tend to be more quenched than that of star-forming centrals. Hence, it seems plausible that halo occupation statistics in which quenched and star forming centrals have different $M_* - M_{\rm h}$ relations could give rise to 2-halo conformity. However, as we demonstrate below, the strength of the effect turns out not to be significant.

Rather than constructing a mock in which we use different $M_* - M_{\rm h}$ relations for quenched and star forming centrals, we demonstrate the inability of different $M_* - M_{\rm h}$ relations to induce 2-halo conformity by comparing the quenched fractions around isolated primaries of different stellar mass. The results, obtained using our standard HOD mock (see § 3.3.1), are shown in Fig. A1, where different symbols correspond to different stellar mass bins, as indicated. The quenched fractions shown are for the entire samples (star-forming plus quenched) of isolated primaries. As is evident, the quenched fraction around isolated primaries correlates very weakly with the stellar mass of the primary. There is a hint for some dependence on small scales ($R < 1.5{\rm Mpc}/h$), but this is barely significant. Hence, even if quenched and star-forming centrals were to have different $M_* - M_{\rm h}$ relations, this would not introduce significant 2-halo conformity. This is easy to understand: in the range of stellar mass considered here, the corresponding host halos are less massive than the redshift-zero collapse mass, which implies that halo bias is only a weak function of halo mass. Based on these findings, and on those described in the main text, we conclude that *the 2-halo conformity signal detected by K13 in SDSS data highlights a generic failure of halo occupation models in which the quenching statistics are governed by halo mass alone.*

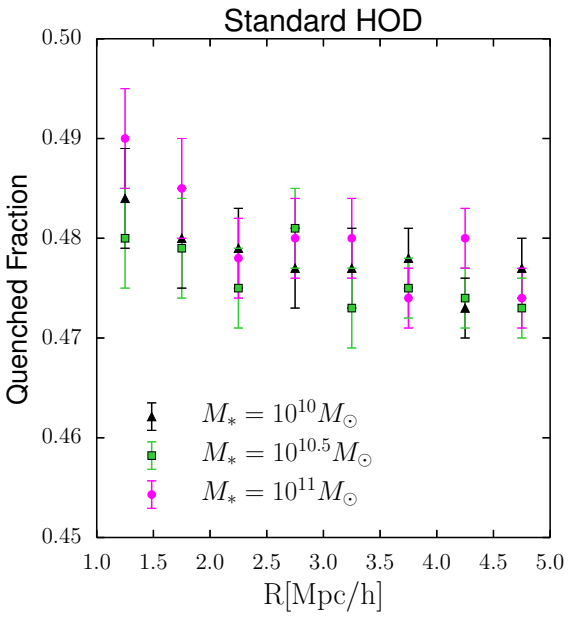


**Figure A1.** The quenched fraction around isolated primary samples of different stellar mass. Isolated primaries have *not* been split into star-forming and quenched subpopulations. This figure shows that the shortcoming of the HOD shown in the top panel of Fig. 2 cannot be resolved by allowing quenched and star-forming populations to have distinct $M_* - M_{\rm halo}$ relations.